Micromegas for Particle Flow Calorimetry

C. Adloff, M. Chefdeville*, **A. Dalmaz, C. Drancourt, R. Gaglione, N. Geffroy, J. Jacquemier, Y. Karyotakis, I. Koletsou, F. Peltier, J. Samarati, G. Vouters**
LAPP, Laboratoire d'Annecy-le-Vieux de Physique des Particules, Université de Savoie, CNRS/IN2P3, 9 Chemin de Bellevue - BP 110, 74941 Annecy-le-Vieux Cedex, France
E-mail: chefdevi@lapp.in2p3.fr

Gaseous sampling hadron calorimeters can be finely segmented and used to record showers with high spatial resolution. This imaging power can be exploited at a future linear collider experiment where the reconstruction of jets by a Particle Flow method will rely on the tracking capability of the calorimeters. Various detector options for this calorimeter are studied within the CALICE collaboration, among which the micro-mesh gaseous structure or Micromegas.

The benefit of Micromegas for digital calorimetry is motivated first, on the basis of a Monte Carlo study. Then, the main features of $1 \times 1\,\mathrm{m}^2$ prototypes with 2-bit embedded readout electronics are presented, together with some selected results from beamtests inside the CALICE steel RPC-SDHCAL.

Calorimetry for High Energy Frontiers - CHEF 2013,
April 22-25, 2013
Paris, France

*Speaker.

1. Introduction

The detailed study of electroweak symmetry breaking and of the properties of the Higgs boson within and beyond the Standard Model (SM) are some of the physics goals motivating the construction of a linear electron positron collider (ILC or CLIC [1, 2]). This physics case is now enhanced with the discovery at LHC of a Higgs-like new particle [3, 4]. Many interesting physics channels at a linear collider will be reconstructed in multi-jet final states, often accompanied by charged leptons and missing transverse energy associated with neutrinos or possibly the lightest super-symmetric particles. The reconstruction of the invariant masses of two or more jets will be important for event reconstruction and event identification. The dijet mass resolution should be good enough to identify Z and W bosons in their hadronic final states with an accuracy comparable to their natural decay width. This requires an excellent jet energy resolution of 3–4 % over an energy range extending up to 1.5 TeV for a 3 TeV collider.

A technique explored by the CALICE [5] collaboration to meet this goal is the Particle Flow. It relies on highly segmented calorimeters and a precise tracker to separate the jet's charged and neutral components [6]. The use of the tracking information reduces the dependence on hadronic calorimetry and results in the required excellent jet energy and di-jet mass resolution [7].

2. Digital calorimetry

2.1 CALICE hadron calorimeters

Two hadron calorimeters are developed by the the CALICE collaboration. The first is instrumented with $3 \times 3\,\mathrm{cm}^2$ scintillating tiles read out by SiPM and 12 bit ADCs [8]. The second uses gaseous detectors with higher segmentation ($1 \times 1\,\mathrm{cm}^2$) and simpler readout (1 bit or 2 bit [9, 10]). The first favours single hadron energy resolution (higher sampling fraction, analogue readout) while the second targets a high shower separation capability (smaller cells) probably at the expense of resolution (digital readout).

A digital hadron calorimeter (1 bit, DHCAL) is expected to have two regimes of operation. A low energy linear regime where the response to the electromagnetic and hadronic shower parts, taken separately, is constant. In this regime, Landau fluctuations are suppressed resulting in improved resolution with respect to a perfect analogue readout. A higher energy saturated regime where the energy information is lost due to under-counting and the resolution degrades with increasing hadron energy [11, 12]. The energy frontier between the two regimes depends mainly on the cell size and absorber material. In an SiD-like HCAL geometry [13] ($1 \times 1\,\mathrm{cm}^2$ pads, steel absorbers), Monte Carlo studies indicate a frontier between 20–30 GeV (cf. section 2.2).

The electromagnetic part of hadron showers results in dense energy deposits and is responsible for the saturation of a DHCAL. A way to account for these deposits in the energy reconstruction is to use additional readout thresholds (2 bit, semi-digital HCAL or SDHCAL). With the right threshold settings and energy reconstruction algorithm, it should be possible to improve the energy resolution beyond the saturated regime.

2.2 Monte Carlo study

Predictions made in the previous section are drawn on the basis of a Monte Carlo study performed with Geant4. The pion response of a Fe/Ar digital calorimeter has been derived over an energy range of 5–70 GeV using samples of 10^4 events per energy. The calorimeter dimensions are such that side are rear leackage are negligible over the studied energy range (Table 1).

N_{layer}	Depth ($\lambda_{int,steel}$)	Transverse area (cm^2)	steel / gas thickness (mm)	Cell size (cm^2)
100	11	100×100	19 / 3	1×1

Table 1: Parameters of the simulated calorimeter.

For each event, the energy deposited in the calorimeter cells by the shower secondary particles is converted into a number of hits by applying a threshold equal to the ionisation potential of the gas. The detector response is not simulated as the amplification process in Micromegas is proportional and the electron diffusion is small compared to the cell size. The number of hits for higher thresholds is determined as well (*e.g.* 5 and 15 MIPs). In this case, the threshold energy corresponding to 1 MIP is deduced from the simulated Landau muon distribution.

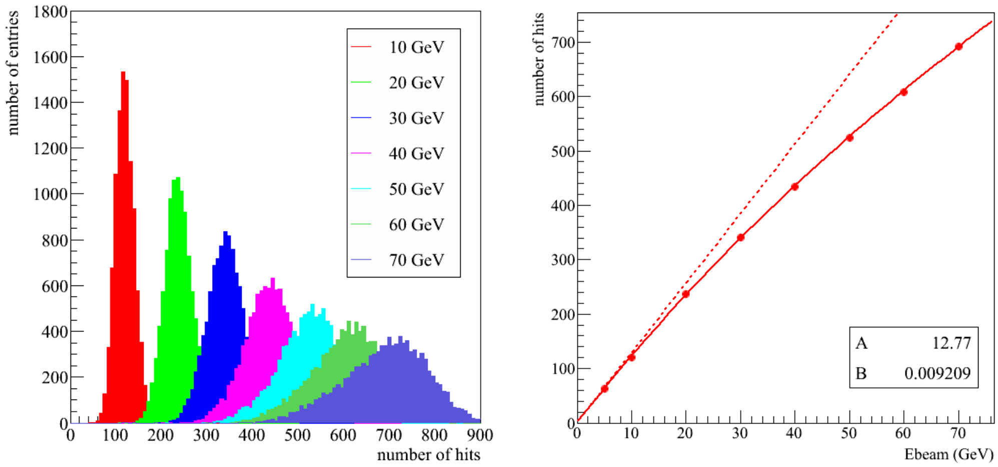

Figure 1: (*left*) N_{hit} distribution from pions showering in an Fe/Ar DHCAL. (*right*) Pion response.

The distribution of the number of hits is showed in Figure 1 (left) for various pion energies and for the lowest threshold. Below 20–30 GeV, the distribution is close to gaussian while above, it develops a left-hand tail due to the fact that the average number of particles per cell increases. Mainly because of this saturation effect, the pion response $N(E_{beam})$ is not a linear function of the pion energy (Figure 1 (right)). It is however well described by the following logarithmic function:

$$N(E_{beam}) = A/B \, \log(1 + BE_{beam}) \tag{2.1}$$

where A is the number of hits per unit energy without saturation and B accounts for the saturation. Adjusting these parameters to the lowest threshold response one finds $A \approx 12.8$ hit / GeV and $B \approx 0.009$ GeV^{-1}. Equation 2.1 is easily inverted to reconstruct the hadron energy in an event j:

$$E^j_{rec}(N) = 1/B \, (\exp(B/A \cdot N^j) - 1) \tag{2.2}$$

The mean and rms of the reconstructed energy distribution are used to calculate the deviation from linearity and energy resolution of the calorimeter. As showed in Figure 2 (left), the energy resolution degrades above 20–30 GeV due to the saturation and can not be described by the usual quadratic sum of a stochastic and constant term.

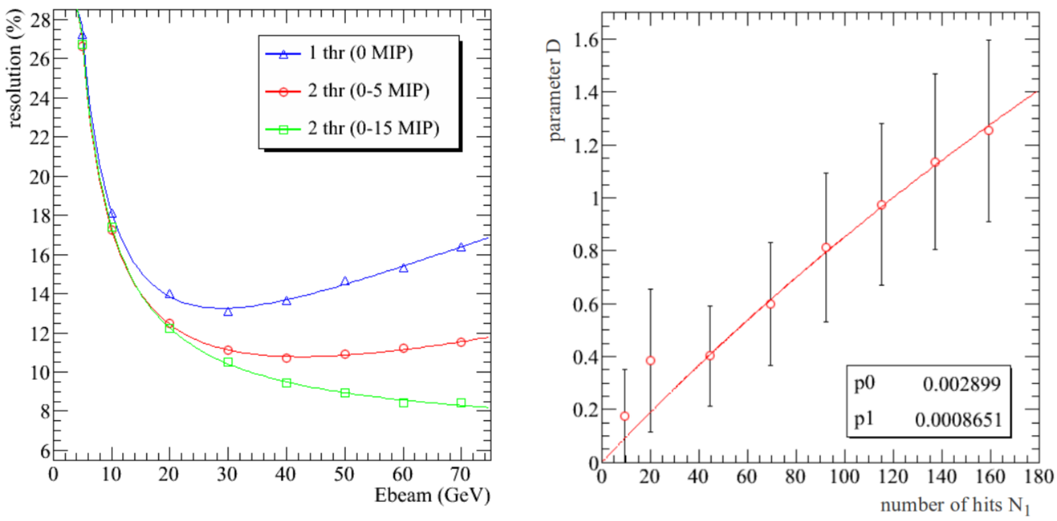

Figure 2: (*left*) Energy resolution in pure digital mode (1 thr) and after applying corrections based on one additional threshold (2 thr). (*right*) Dependence of the high threshold weight on the number of hits above this threshold (error bars are equal to the rms of the weight).

As mentioned previously, the degradation of the resolution can be mitigated by identifying cells with larger energy deposits (*i.e.* with signals passing higher thresholds) and adding corrections to the reconstructed energy. Using two readout thresholds, the hadron energy can be written:

$$E^j_{\text{rec}}(N_0, N_1) = C(N^j_0 + D\, N^j_1) \tag{2.3}$$

where N^j_0 and N^j_1 are the number of hits above the low and high threshold in event j . The parameter C converts a number of hits into energy and identifies to $1/A \sim 0.08$ GeV / hit. The parameter D is the weight of the high threshold and should be energy dependent. It is determined by requiring that the average reconstructed energy is equal to the hadron energy ($E_{\text{rec}} = E_{\text{beam}}$) which translates into:

$$D(E_{\text{beam}}) = 1/N_1\ (AE_{\text{beam}}\ -\ N_0) \tag{2.4}$$

The simulation indicates that D is close to a monotonically increasing function of E_{beam} over the studied energy range. It is also the case of $N_1(E_{\text{beam}})$ and therefore of $D(E_{\text{beam}})$. This dependence can be parametrised (Figure 2 (right)) and used to reconstruct the hadron energy using Equation 2.3. The energy resolution obtained with a high threshold of 5 and 15 MIPs is shown is Figure 2 (left). In the first case (5 MIP), the resolution improves beyond 20–30 GeV and degrades above 50-60 GeV. With a 15 MIP threshold, no degradation occurs at least up to 70 GeV. With this reconstruction algorithm, deviations from linearity are below ± 2 % over the studied energy range. More sophisticated algorithms would likely yield event better results. This simple one, however, is sufficient to emphasize the limitation of a single threshold calorimeter.

3. Micromegas prototypes

In order to perform tests inside the CALICE SDHCAL steel structure and demonstrate the technical feasability of large Micromegas chambers, 4 prototypes of $1 \times 1\,\text{m}^2$ have been constructed [14]. The key of the design is the integration of the front-end readout chips on the detector printed circuits boards. The latter also houses the anode pads ($1 \times 1\,\text{cm}^2$) and the mesh. With this design, the prototype thickness is kept to ~ 1 cm and dead zones below 2 % of the total active area.

The readout chip is called MICROROC and features 64 channels with a low noise preamplifier, 2 shapers of different gain, 3 discriminators (*i.e.* 3 thresholds) and a 127 event depth memory [15]. In typical operating conditions (gas gain of $\sim 10^3$), the smallest detectable signal is ~ 0.2 MIP (1–2 fC) and the behaviour of the shapers is linear up to 40 and 100 MIPs (200 and 500 fC). Designed for an application at the ILC, the MICROROC also features timestamping of hits (5 MHz clock), self-triggering and power-pulsing capability. Each $1 \times 1\,\text{m}^2$ prototype is equipped with 9216 anode pads and therefore with 144 MICROROC chips.

4. Testbeam results

Micromegas prototypes of $1 \times 1\,\text{m}^2$ were inserted inside the CALICE SDHCAL steel structure together with RPCs of similar size and electronics [16]. The structure is a 50 layer sandwich of steel absorbers and air gaps ($\sim 5.5\,\lambda_{\text{int}}$). It was installed at the CERN/SPS beam facility and equipped with 2 Micromegas in May and 4 in November, the remaining slots being filled with RPCs. Thanks to a common data acquisition system, full offline event reconstruction was possible.

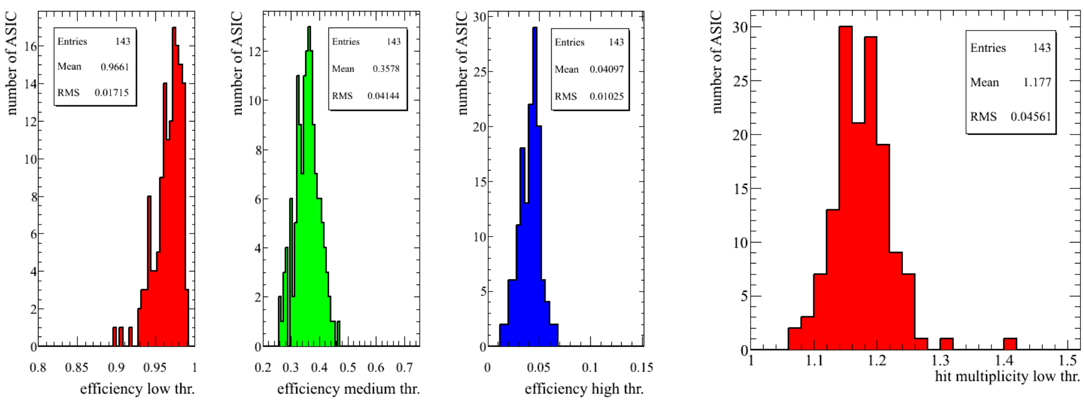

Figure 3: (*left*) Efficiency for the low, medium and high threshold measured over the total area of one prototype in $8 \times 8\,\text{cm}^2$ regions. (*right*) Hit multiplicity for the low threshold.

The efficiency of the 3 thresholds to MIPs was measured with a 100 GeV muon beam for all the MICROROC chips of one prototype (in $8 \times 8\,\text{cm}^2$ regions). With the thresholds set at (0.25 , 2 , 10) MIPs, an average efficiency of (96.6 , 35.7 , 4.1) % was measured with small chip-to-chip dispersion of (1.8 , 4.2 , 1.1) % RMS (Figure 3 (left)). The average hit multiplicity is below 1.2 for the low threshold and decreases further for higher thresholds ((Figure 3 (right)). These very good results are achieved thanks to a precise calibration of the MICROROCs and a good uniformity of the Micromegas chamber response.

An important measurement with pions became possible with 4 Micromegas prototypes and 46 RPCs inside the SDHCAL. By spotting the layer at which the shower starts, the (average) longitudinal profile can be measured using only the information from the Micromegas equipped layers, namely layer number 10, 20, 35 and 50 (Figure 4 left). Furthermore, the average number of hits that would be measured with a fully Micromegas equipped SDHCAL can be calculated as the integral of the profile from 0 to infinity using a proper fit function. This analysis was applied to several pion samples at various energies (from 20 GeV to 150 GeV) and allowed a measurement of the response of a virtual Micromegas SDHCAL, for the 3 thresholds (Figure 4 right). Adjusting the parameters A and B of Equation 2.1 to the measured response, a good agreement is found between experimental and Monte Carlo simulation data. This conclusion is preliminary and a more detailed analysis is on-going.

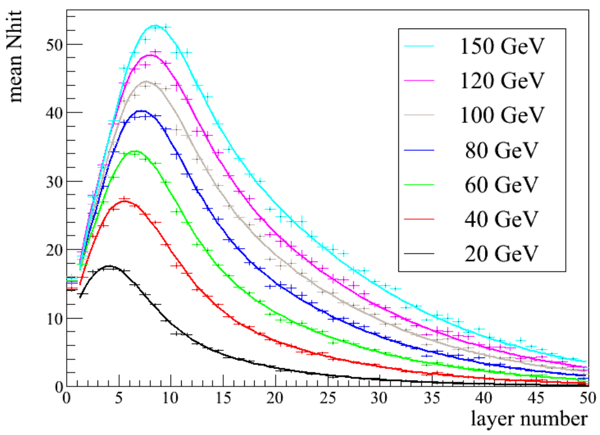

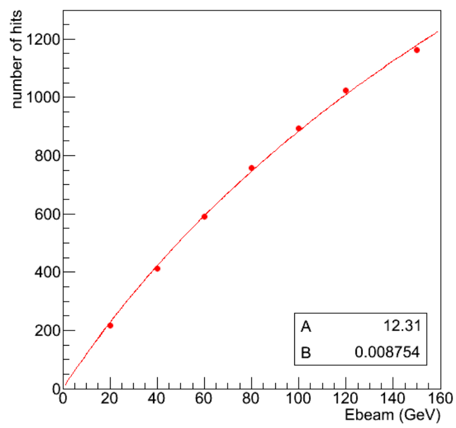

Figure 4: (*left*) Longitudinal pion shower profile in a virtual Micromegas SDHCAL as measured with 4 prototypes inside the CALICE steel RPC-SDHCAL. (*right*) Pion response deduced from the profiles.

5. Conclusion

The energy resolution of a highly segmented gaseous calorimeter with digital readout can probably greatly benefit from the use of at least one additional threshold. In that respect, Micromegas is a very appealing choice for the active layers of this calorimeter as it is free of space charge effects and delivers proportional signals. Large size prototypes ($1 \times 1\ m^2$) fabricated up to now are equipped with a dedicated front-end electronics featuring 3 thresholds. Extensive tests in particle beams reveal excellent performance to MIPs as well as in hadron showers. They also provide high precision data for testing and improving simulation programs of hadron showers.

If a full Micromegas SDHCAL prototype is to be built in the future, improvement of the chamber design could be realised before. For instance by replacing the numerous discharge protection diode networks soldered on the ASIC boards by resistive coatings applied directly onto the anode pads. Small prototypes will soon become available and will be the subject of further tests in particle beams.

References

[1] James Brau, Yasuhiro Okada, Nicholas J. Walker, Abdelhak Djouadi, Joseph Lykken, et al. International Linear Collider reference design report. 1: Executive summary. 2: Physics at the ILC. 3: Accelerator. 4: Detectors. 2007.

[2] E. Accomando et al. Physics at the CLIC multi-TeV linear collider. 2004.

[3] Georges Aad et al. Observation of a new particle in the search for the Standard Model Higgs boson with the ATLAS detector at the LHC. *Phys.Lett.*, B716:1–29, 2012.

[4] S. Chatrchyan et al. Observation of a new boson at a mass of 125 GeV with the CMS experiment at the LHC. *Physics Letters B*, 716(1):30 – 61, 2012.

[5] The calice collaboration, https://twiki.cern.ch/twiki/bin/view/calice.

[6] Jean-Claude Brient and Henri Videau. The Calorimetry at the future e+ e- linear collider. *eConf*, C010630:E3047, 2001.

[7] M.A. Thomson. Particle Flow Calorimetry and the PandoraPFA Algorithm. *Nucl.Instrum.Meth.*, A611:25–40, 2009.

[8] V. Andreev, V. Balagura, B. Bobchenko, P. Buzhan, J. Cvach, et al. A high granularity scintillator hadronic-calorimeter with SiPM readout for a linear collider detector. *Nucl.Instrum.Meth.*, A540:368–380, 2005.

[9] Burak Bilki, John Butler, Tim Cundiff, Gary Drake, William Haberichter, et al. Calibration of a digital hadron calorimeter with muons. *JINST*, 3:P05001, 2008.

[10] S. Mannai, K. Manai, Y. Haddad, I. Laktineh, and E. Cortina. High granularity Semi-Digital Hadronic Calorimeter using GRPCs. *Nucl.Instrum.Meth.*, A718:91–94, 2013.

[11] A. Ghezzi, T. Tabarelli de Fatis, G. Tinti, and M. Piccolo. Digital hadron calorimetry with glass RPC active detectors. *eConf*, C050318:0928, 2005.

[12] Catherine Adloff, Jan Blaha, Jean-Jaques Blaising, Maximilien Chefdeville, Ambroise Espargiliere, et al. Monte carlo study of the physics performance of a digital hadronic calorimeter. *JINST*, 4:P11009, 2009.

[13] H. Aihara, P. Burrows, M. Oreglia, E.L. Berger, V. Guarino, et al. SiD Letter of Intent. 2009.

[14] C. Adloff, J. Blaha, J.-J. Blaising, M. Chefdeville, A. Dalmaz, et al. Construction and test of a $1\times1\text{m}^2$ Micromegas chamber for sampling hadron calorimetry at future lepton colliders. *Nucl.Instrum.Meth.*, A729:90–101, 2013.

[15] C. Adloff, J. Blaha, M. Chefdeville, A. Dalmaz, C. Drancourt, et al. MICROROC: MICRO-mesh gaseous structure Read-Out Chip. *JINST*, 7:C01029, 2012.

[16] Robert Kieffer. Development of a semi-digital hadronic calorimeter using GRPCs for future linear collider experiments. *Nucl.Instrum.Meth.*, A628:328–331, 2011.